

# UC Irvine

## UC Irvine Previously Published Works

### Title

Prophylactic evaluation of verubecestat on disease- and symptom-modifying effects in 5XFAD mice

### Permalink

<https://escholarship.org/uc/item/08m5g6f5>

### Journal

Alzheimer's & Dementia: Translational Research & Clinical Interventions, 8(1)

### ISSN

2352-8737

### Authors

Oblak, Adrian L  
Cope, Zackary A  
Quinney, Sara K  
et al.

### Publication Date

2022

### DOI

10.1002/trc2.12317

Peer reviewed

## RESEARCH ARTICLE

# Prophylactic evaluation of verubecestat on disease- and symptom-modifying effects in 5XFAD mice

Adrian L. Oblak<sup>1</sup> | Zackary A. Cope<sup>2</sup> | Sara K. Quinney<sup>1</sup> | Ravi S. Pandey<sup>3,4</sup> |  
Carla Biesdorf<sup>1</sup> | Andi R. Masters<sup>1</sup> | Kristen D. Onos<sup>5</sup> | Leslie Haynes<sup>5</sup> |  
Kelly J. Keezer<sup>5</sup> | Jill A. Meyer<sup>1</sup> | Jonathan S. Peters<sup>1</sup> | Scott A. Persohn<sup>1</sup> |  
Amanda A. Bedwell<sup>1</sup> | Kierra Eldridge<sup>1</sup> | Rachael Speedy<sup>1</sup> | Gabriela Little<sup>2</sup> |  
Sean-Paul Williams<sup>2</sup> | Brenda Noarbe<sup>5</sup> | Andre Obenaus<sup>5</sup> | Michael Sasner<sup>4</sup> |  
Gareth R. Howell<sup>3,5</sup> | Gregory W. Carter<sup>3,5</sup> | Harriet Williams<sup>4</sup> | Bruce T. Lamb<sup>1</sup> |  
Paul R. Territo<sup>1</sup> | Stacey J. Sukoff Rizzo<sup>2,4</sup>

<sup>1</sup>Indiana University School of Medicine,  
Indianapolis, Indiana, USA

<sup>2</sup>University of Pittsburgh School of Medicine,  
Pittsburgh, Pennsylvania, USA

<sup>3</sup>The Jackson Laboratory for Genomic  
Medicine, Farmington, Connecticut, USA

<sup>4</sup>The Jackson Laboratory, Bar Harbor, Maine,  
USA

<sup>5</sup>University of California, Irvine, California,  
USA

## Correspondence

Adrian L. Oblak, Indiana University School of  
Medicine, Stark Neurosciences Research  
Institute, 320 W. 15<sup>th</sup> Street, NB 108B,  
Indianapolis, IN 46202, USA.  
Email: [aoblak@iu.edu](mailto:aoblak@iu.edu)

## Abstract

**Introduction:** Alzheimer's disease (AD) is the most common form of dementia. Beta-secretase (BACE) inhibitors have been proposed as potential therapeutic interventions; however, initiating treatment once disease has significantly progressed has failed to effectively stop or treat disease. Whether BACE inhibition may have efficacy when administered prophylactically in the early stages of AD has been under-investigated. The present studies aimed to evaluate prophylactic treatment of the BACE inhibitor verubecestat in an AD mouse model using the National Institute on Aging (NIA) resources of the Model Organism Development for Late-Onset Alzheimer's Disease (MODEL-AD) Preclinical Testing Core (PTC) Drug Screening Pipeline.

**Methods:** 5XFAD mice were administered verubecestat ad libitum in chow from 3 to 6 months of age, prior to the onset of significant disease pathology. Following treatment (6 months of age), in vivo imaging was conducted with 18F-florbetapir (AV-45/Amyvid) (18F-AV45) and 18-FDG (fluorodeoxyglucose)-PET (positron emission tomography)/MRI (magnetic resonance imaging), brain and plasma amyloid beta (A $\beta$ ) were measured, and the clinical and behavioral characteristics of the mice were assessed and correlated with the pharmacokinetic data.

**Results:** Prophylactic verubecestat treatment resulted in dose- and region-dependent attenuations of 18F-AV45 uptake in male and female 5XFAD mice. Plasma A $\beta$ 40 and A $\beta$ 42 were also dose-dependently attenuated with treatment. Across the dose range evaluated, side effects including coat color changes and motor alterations were reported, in the absence of cognitive improvement or changes in 18F-FDG uptake.

This is an open access article under the terms of the [Creative Commons Attribution-NonCommercial-NoDerivs](https://creativecommons.org/licenses/by-nc-nd/4.0/) License, which permits use and distribution in any medium, provided the original work is properly cited, the use is non-commercial and no modifications or adaptations are made.

© 2022 The Authors. *Alzheimer's & Dementia: Diagnosis, Assessment & Disease Monitoring* published by Wiley Periodicals, LLC on behalf of Alzheimer's Association.

**Discussion:** Prophylactic treatment with verubecestat resulted in attenuated amyloid plaque deposition when treatment was initiated prior to significant pathology in 5XFAD mice. At the same dose range effective at attenuating A $\beta$  levels, verubecestat produced side effects in the absence of improvements in cognitive function. Taken together these data demonstrate the rigorous translational approaches of the MODEL-AD PTC for interrogating potential therapeutics and provide insight into the limitations of verubecestat as a prophylactic intervention for early-stage AD.

**KEYWORDS**

amyloid, BACE inhibitor, MODEL-AD, mouse model, preclinical testing

## 1 | INTRODUCTION

Alzheimer's disease (AD) is the most common form of dementia worldwide, and the number of affected individuals in the United States is expected to near 14 million by 2050.<sup>1</sup> There are currently no effective strategies to prevent or reverse AD onset,<sup>2,3</sup> despite extensive research studies and clinical trials in recent years costing over \$3 billion USD.<sup>4,5</sup> Approximately 99% of potential AD therapeutics have proven ineffective in clinical trials.<sup>4,5</sup>

Several clinical trials have investigated the use of beta-secretase (BACE) inhibitors as AD therapeutics,<sup>6,7</sup> based on the premise of the amyloid hypothesis, which postulates the accumulation of amyloid beta (A $\beta$ ) as the primary driving factor of AD pathology,<sup>6-8</sup> and data indicating that a lack of BACE does not have an adverse effect on the brain in mice.<sup>9</sup> BACE cleaves amyloid precursor protein (APP) in neurons, generating soluble A $\beta$ 40 and A $\beta$ 42 peptides that form aggregates in the AD brain.<sup>10</sup> Consequently, it was proposed that BACE inhibition would, in turn, reduce the generation of these peptides and oligomers, thereby reducing A $\beta$  plaque formation, thus ameliorating AD.<sup>6,7</sup> To date, several BACE inhibitor clinical trials have been halted due to adverse events or lack of clinical efficacy despite lowering A $\beta$ .<sup>7</sup> However, most of these clinical trials focused on late-stage AD, in which significant A $\beta$  plaque accumulation has already occurred.<sup>7</sup> Continued interest remains in the potential efficacy of BACE inhibitors if administered prior to the onset of symptoms in patients identified as at risk for developing AD or in early stages of AD.<sup>7</sup> In investigate whether BACE inhibition is a viable prospect as an AD therapeutic in a prophylactic context, preclinical studies incorporating translational outcome measures are needed. In this respect, to investigate the potential of a prophylactic approach, we utilized the recently established drug-screening resources of the Model Organism Development for Late-Onset Alzheimer's Disease (MODEL-AD) Preclinical Testing Core (PTC).<sup>11</sup>

The MODEL-AD PTC was established to conduct streamlined preclinical drug testing that rigorously evaluates candidate compounds using a tiered screening strategy with well-defined go/no-go criteria for advancement and prioritization of translational assays and outcome measures.<sup>11</sup> For the present studies, we selected the 5XFAD mouse model to evaluate the pharmacokinetic, pharmacodynamic,

and functional profile of the BACE-1 inhibitor verubecestat administered chronically prior to the onset of significant AD pathology. The 5XFAD model was selected given its well-characterized trajectory of early and significant amyloid plaque deposition, and was therefore an appropriate model for evaluating in vivo target engagement and functional consequences of BACE1 inhibition.<sup>12</sup> The goal of these studies was to investigate whether prophylactic treatment with verubecestat would slow or prevent disease and improve the side-effect profile reported previously with treatment initiated in moderate and later stages of disease.<sup>13-15</sup> Findings from these studies may provide insight into a clinical path for investigating BACE inhibition as a preventative strategy to slow or prevent AD.

## 2 | METHODS

Detailed methods are included in the supporting information, and all standard operating procedures and raw data are available via the AD Knowledge Portal: <https://adknowledgeportal.org>.

### 2.1 | Subjects and housing conditions

These studies conform to the Guide for the Care and Use of Laboratory Animals published by the National Institutes of Health (NIH Publication No. 85-23, revised 2011) and were reviewed and approved by the respective Institutional Animal Care and Use Committees (IACUC) at Indiana University (IU), The Jackson Laboratory (JAX), and The University of Pittsburgh (PITT) prior to study initiation.

5XFAD mice on a congenic C57BL/6J background, which have been extensively characterized by the IU/JAX/PITT MODEL-AD Center,<sup>12</sup> were used for these studies. 5XFAD mice overexpress human APP and five familial AD gene mutations including three in APP and two in PSEN1 (K670N/M671L, I716V, V717I, M146L, and L286V).<sup>16</sup> For these studies, mice were bred at IU and JAX by crossing male 5XFAD (MMRRC ID #34848) with female C57BL6/J (JAX stock #000664), as described previously.<sup>12</sup> In vivo imaging studies were conducted at IU as the primary translational pharmacodynamics (PD) end points, and pilot pharmacokinetics (PK) and in vivo functional studies were

conducted at JAX. Subjects were group housed throughout the study unless otherwise described below. For cross-laboratory reproducibility studies conducted at PITT, assessments included PK evaluation of A $\beta$  in brain and plasma via enzyme-linked immunosorbent assay (ELISA) as a PD end point, and behavioral assessments. At PITT, adult male and female 5XFAD and control mice were ordered from JAX (stock #34848 and #000664) at 8 to 12 weeks of age, group housed within same-sex and same genotype cages, and acclimated for at least 1 week prior to initiating treatment. Across all sites, the light cycle was on a 12:12 light:dark schedule with experiments conducted during the light cycle except for the pilot PK studies, which included sampling throughout the circadian period (see Supplemental Methods). Sample sizes were pre-determined via power analysis based on previously reported characterization data for 5XFAD,<sup>12</sup> and required  $n = 10$  to 15 mice per sex per dose level per tracer for imaging studies and  $n = 10$  to 12 per sex per genotype per dose level for behavioral studies. Verubecestat (VER) treatment started at 3 months of age, for a 3-month duration with terminal studies completed at 6 months of age. Bodyweights were collected every other day for the first week of the study and then weekly for the remainder of the study to confirm no difference between control and VER diet. No pre-treatment imaging was conducted for baseline values in this study. Genotypes and treatments were coded (e.g., A, B, C, etc.) to ensure blinding of technical staff conducting experiments and throughout data analysis, with subjects randomized and counterbalanced in line with the ARRIVE guidelines.<sup>17</sup>

## 2.2 | Chemicals and reagents

Verubecestat (CAS no. 1286770-55-5) and MK-2206 (CAS no. 1032350-13-2) were purchased from Selleck Chemicals (Houston, TX). A bulk synthesis batch of VER was sent to Test Diet (Cincinnati, OH) and milled into chow (LabDiet 5LG4) in the following concentrations: 60, 180, and 600 ppm, which was calculated to provide a daily dosage of 10, 30, and 100 mg/kg/day based on mouse weight and typical consumption of daily chow (see supplemental materials). A sham diet that did not contain verubecestat served as the vehicle control. All diets were irradiated prior to shipping. Prior to the initiation of treatment, diet formulations were sent to the IU Clinical Pharmacology Analytical Core (CPAC) for analysis and confirmation of the active ingredient/concentration of verubecestat (see Supplemental Materials).

## 2.3 | Pilot PK and PK/PD modeling

Initial in vivo PK sampling for verubecestat was conducted at JAX as a pilot PK study in 6-month-old male and female 5XFAD mice. These data were used for chronic dosing simulations to inform the dosing regimen for pharmacodynamics studies. For PK studies with ad libitum drug-milled chow, a protocol was developed to maximize inter-sampling rest periods to ensure that ad libitum feeding returned to steady state after

## RESEARCH IN CONTEXT

- 1. Systematic Review:** The authors reviewed the literature using traditional (e.g., PubMed) sources and meeting abstracts and presentations. Although clinical trials of beta-secretase (BACE) inhibitors for Alzheimer's disease (AD) have failed due to lack of efficacy and adverse events, several recent publications have indicated a need to investigate prophylactic treatment.
- 2. Interpretation of Results:** Our findings indicate that BACE inhibitors, when administered prophylactically, prior to significant amyloid pathology, may have neuroprotective benefit from amyloid accumulation; however, some adverse side effects were still observed, which may be related to the compound investigated.
- 3. Future Directions:** The present studies provide a framework for conducting preclinical translational studies using a prophylactic approach. Further studies are required to support the potential of BACE inhibitors as prophylactic treatments and ideally with compounds that have improved selectivity for BACE1 to minimize potential adverse effects.

each sample collection (see [supplementary methods](#)). Simulations of chronic dosing schedules were conducted in R (v3.4.3) using deSolve<sup>18</sup> (see supplementary materials).

## 2.4 | Chronic verubecestat treatment

Daily treatment was initiated at 3 months of age, with regular chow replaced with the coded diet (e.g., A, B, C, etc.) to ensure blinding. Chow was provided ad libitum, and mice were monitored and weighed daily throughout the first week of treatment and once weekly thereafter to confirm consumption and rule out welfare concerns or taste aversion. Otherwise, mice were undisturbed until testing at 6 months of age with the exception of regular husbandry procedures. Treatment continued through the testing period including on the day of terminal tissue collection.

## 2.5 | Magnetic resonance imaging

Two days prior to positron emission tomography (PET) scanning, mice were anesthetized with isoflurane and T2-weighted (T2W) magnetic resonance (MR) images were acquired using a 3T Siemens Prisma clinical MRI scanner outfitted with a dedicated 4-channel mouse head coil and bed system (RapidMR). Images were acquired using a SPACE3D sequence yielding  $0.18 \times 0.18 \times$

0.2 mm resolution images (see [supplementary methods](#) for sequence details).

## 2.6 | Positron emission tomography (PET) imaging and autoradiography

Each animal (minimum  $n = 10$  mice/sex/dose) was scanned on the Siemens 3T MRI at least 1 to 2 days before PET scanning on the IndyPET3 scanner. For PET imaging, conscious mice were injected with 3.7 to 9.25 MBq (0.1–0.25 mCi) of [18F]-AV45 (i.v.) or [18F]-FDG (i.p.), prior to anesthesia to permit tracer uptake. Post uptake, animals were anesthetized with isoflurane and scanned on the IndyPET3 scanner.<sup>18</sup> Upon completion of PET imaging, calibrated listmode data were reconstructed into a single-static image with a minimum field of view of 60 mm using filtered-back-projection (FBP), and were corrected for decay, random coincidence events, and dead-time loss.<sup>19</sup> Post-mortem brains were sectioned and mounted as described previously<sup>12</sup> and scanned on Typhoon FL 7000IP (GE Medical Systems) phosphor-imager at 25  $\mu$ m resolution.

## 2.7 | PET/MRI and autoradiography analysis

All PET and MRI results were co-registered using a 9 degrees of freedom ridged-body mutual information-based normalized entropy algorithm<sup>20</sup> and mapped to stereotactic mouse brain coordinates<sup>21,22</sup> using Analyze 12 (AnalyzeDirect, Stilwell KS). Post-registration, 56 bilateral regions were extracted, and left and right regions were averaged and ratioed to the cerebellum yielding 27 unique specific uptake value ratio (SUVR) volumes of interest. Regions were subjected to principal component analysis (PCA), where regions that explain the top 80% of variance were analyzed for differences with dose and sex using two-way analysis of variance (ANOVA) (Prism, GraphPad Inc.), where significance was taken at  $P < .05$ .

To assess brain volume, the atlas was applied to a model brain from the Paxinos-Franklin stereotactic brain atlas using Analyze 12.0 for registration. Regional labels were applied to each animal's T2 scan with Advanced Normalization Tools (ANTs),<sup>23</sup> and voxel volumes (mm<sup>3</sup>) were extracted using ITK-SNAP.<sup>24</sup> Nested ANOVA statistics was conducted in Prism using sex and dose levels as factors, where the primary change was based on sex and the second was sex by dose, to see if there were dose-dependent changes.

## 2.8 | Plasma and brain multi-plex A $\beta$ ELISA

Soluble and insoluble fractions from hemi-brain homogenates (minus cerebellum) were prepared by diethanolamine (DTT) and formic acid extraction, respectively, like methods previously described<sup>12,26</sup> (see [supplementary methods](#)). A $\beta$ 40 and 42 were analyzed in brain fractions and plasma using the vPLEXA $\beta$  Peptide Panel 1 (4G8) (MesoScale Diag-

nostics #K15199E) in accordance with the manufacturer's supplied protocol, with brain normalized for total protein.

## 2.9 | Behavioral assessments

The behavioral testing for the present studies included assays in which 5XFAD typically demonstrate a phenotype relative to wild-type controls,<sup>12</sup> and assays to capture parameters that have been previously reported in clinical trials, including spatial working memory, risk of falls, and adverse events.<sup>13–15</sup> For these studies, following 12 weeks of daily treatment, behavioral tests were conducted at JAX and PITT as reported previously<sup>12,25</sup> in the following order with at minimum a 1 to 2 day rest period between tests: open field test, spontaneous alternation, rotarod, and an additional frailty assessment conducted at PITT (see [supplementary methods](#)). Behavioral data were analyzed by genotype within sex by one-way or two-way ANOVA as appropriate versus sex- and age-matched vehicle-treated 5XFAD controls.

## 2.10 | Transcriptomic analysis

Similar to as described previously,<sup>12</sup> total RNA was extracted from frozen right brain hemispheres using the MagMAX mirVana Total RNA Isolation Kit (ThermoFisher) and the KingFisher Flex purification system (ThermoFisher, Waltham, MA). RNA concentration and quality were assessed using the Nanodrop 2000 spectrophotometer (Thermo Scientific) and the RNA Total RNA Nano assay (Agilent Technologies, Santa Clara, CA). The NanoString Mouse AD gene expression panel was used for gene expression profiling on the nCounter platform (NanoString, Seattle, WA) as described by the manufacturer. nSolver software was used for analysis of NanoString gene expression values.

## 2.11 | Data processing

PK data were unblinded to confirm drug exposure, whereas the blind was maintained throughout analysis of PD and behavioral measures with only subjects that met a priori exclusion criteria removed (e.g., drug detected in control subjects; see supplemental materials). Subjects were not excluded by any mathematical determination as an outlier (e.g., two standard deviations [SD]). (Detailed analysis and data processing for each assay are described in the supplementary materials.) Genotypes from terminal tail tip collection were confirmed prior to unblinding.

## 3 | RESULTS

### 3.1 | Pharmacokinetics data and PK/PD modeling

Quality control (QC) analysis of the drug formulated in chow revealed high inter- and intra-pellet variability with lower-than-expected

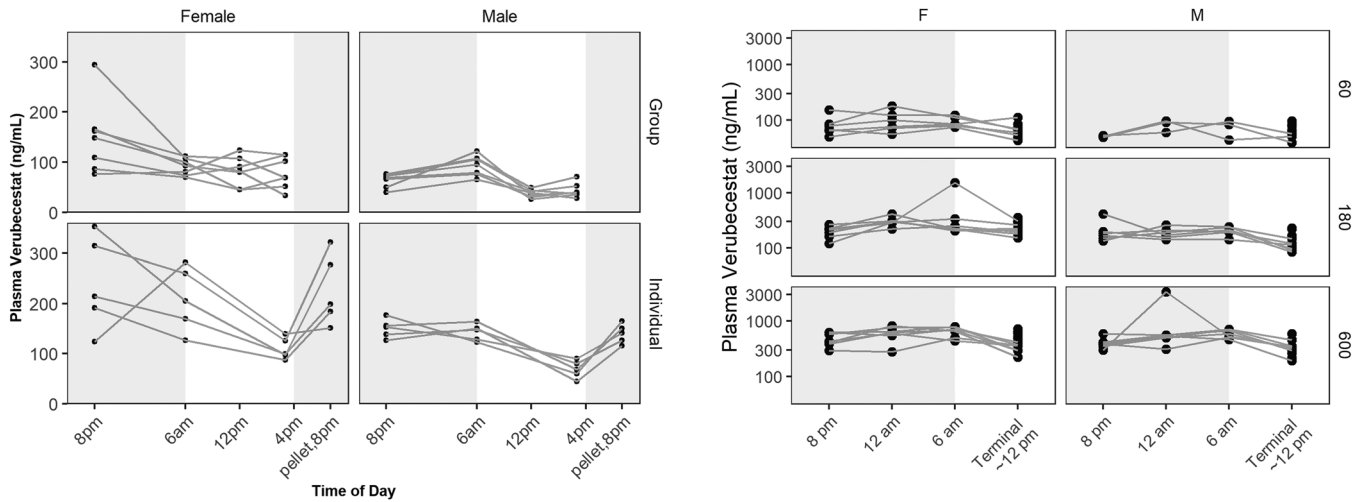


**FIGURE 1** Pilot pharmacokinetic data in 6-month-old 5XFAD male and female mice. Plasma concentrations of verubecestat following ad libitum feeding in chow containing 60 ppm verubecestat trifluoroacetate in group- ( $N = 2$  and  $N = 5$  mice per cage per sex, top) or individually ( $N = 5$  per sex, bottom) housed 5XFAD mice. Fresh pulverized chow was placed on the cage floor at 4 pm daily. Right panel: Verubecestat plasma concentrations following chronic treatment with chow containing verubecestat at 60, 180, and 600 parts per million (ppm). Lights were off from 6 pm to 6 am, indicated by the shaded region. Blood samples were obtained on separate days, as described in Materials and Methods.

concentrations (see Supplemental Materials). Analysis of plasma samples from the pilot PK data (Table S1) were used to inform the chronic dosing regimen. As illustrated in Figure 1, plasma concentrations were variable in all dose and sex groups within and across sites. In addition, plasma concentrations in mice treated at IU were slightly lower than those from JAX and PITT. Females demonstrated higher concentrations than males. Brain concentrations were  $\approx 20\%$  of plasma concentrations in mice from JAX and 9% to 24% of plasma concentrations in mice from PITT. In general, exposures were in line with literature reports for in vivo target engagement.<sup>26,27</sup>

### 3.2 | Amyloid accumulation in 5XFAD mice treated with verubecestat

Prophylactic verubecestat treatment resulted in dose-dependent reductions in 18F-AV45 uptake in a region-dependent manner. In both male and female 5XFAD mice, 18F-AV45 uptake was significantly ( $P < .05$ ) reduced as a function of increasing verubecestat dose, increased in memory, integration, sensory, and motor regions (Figure 2), consistent with clinical imaging finding for verubecestat. Fourteen additional regions not presented did not show dose-related effects. Confirmational autoradiographic analysis support these findings and showed similar levels of changes across the same brain regions (Figure S1) which were confirmed via ThioS staining (Figure S1).

Analysis of A $\beta$ 40 and A $\beta$ 42 in hemibrain and plasma measured via ELISA is presented in Figure 3. As expected, vehicle-treated 5XFAD male and female mice demonstrated increases in A $\beta$ 40 and A $\beta$ 42 relative to age- and sex-matched vehicle-treated C57BL/6J controls for

brain and plasma measures ( $P < .05$ ). Prophylactic treatment with verubecestat resulted in reduced plasma A $\beta$ 40 and A $\beta$ 42 in both male and female mice. In soluble brain fraction, prophylactic verubecestat treatment attenuated A $\beta$ 40 and A $\beta$ 42 in female mice across the dose range; however, only modest reductions were observed in male mice and only at the highest dose tested. Of interest, in the insoluble fraction, the lowest dose of verubecestat demonstrated modest reductions in A $\beta$ 40 and A $\beta$ 42 only in female mice, whereas in male mice, the lowest dose increased A $\beta$ 40 and A $\beta$ 42 levels, while higher doses were not significantly different than vehicle treated controls ( $P > .05$ ).

### 3.3 | 18-FDG PET uptake and volumetric changes in 5XFAD mice treated with verubecestat

Prophylactic treatment with verubecestat at the dose range tested did not alter 18F-FDG (fluorodeoxyglucose) uptake for any region studied as presented in Figure 4 and was consistent with previous reports in clinic. Confirmational autoradiographic analysis showed no change in 18F-FDG uptake across regions, sexes, and doses (Figure S2). Post-mortem staining and immunohistochemistry were completed as a conformational readout of the amyloid deposition changes, which were validated by ThioS staining. In addition, glycolytic changes, which are driven largely by microglia metabolic reprogramming during amyloid clearance<sup>28,29</sup> were confirmed by ionized calcium-binding adaptor protein-1 (IBA1) staining (Figure S2).

Given the lack of changes in regional glycolytic metabolism as measured by PET, volumetric changes throughout the brain were also measured. No change in volumes were observed, however, as a function of sex, region, or dose (Figure S3).



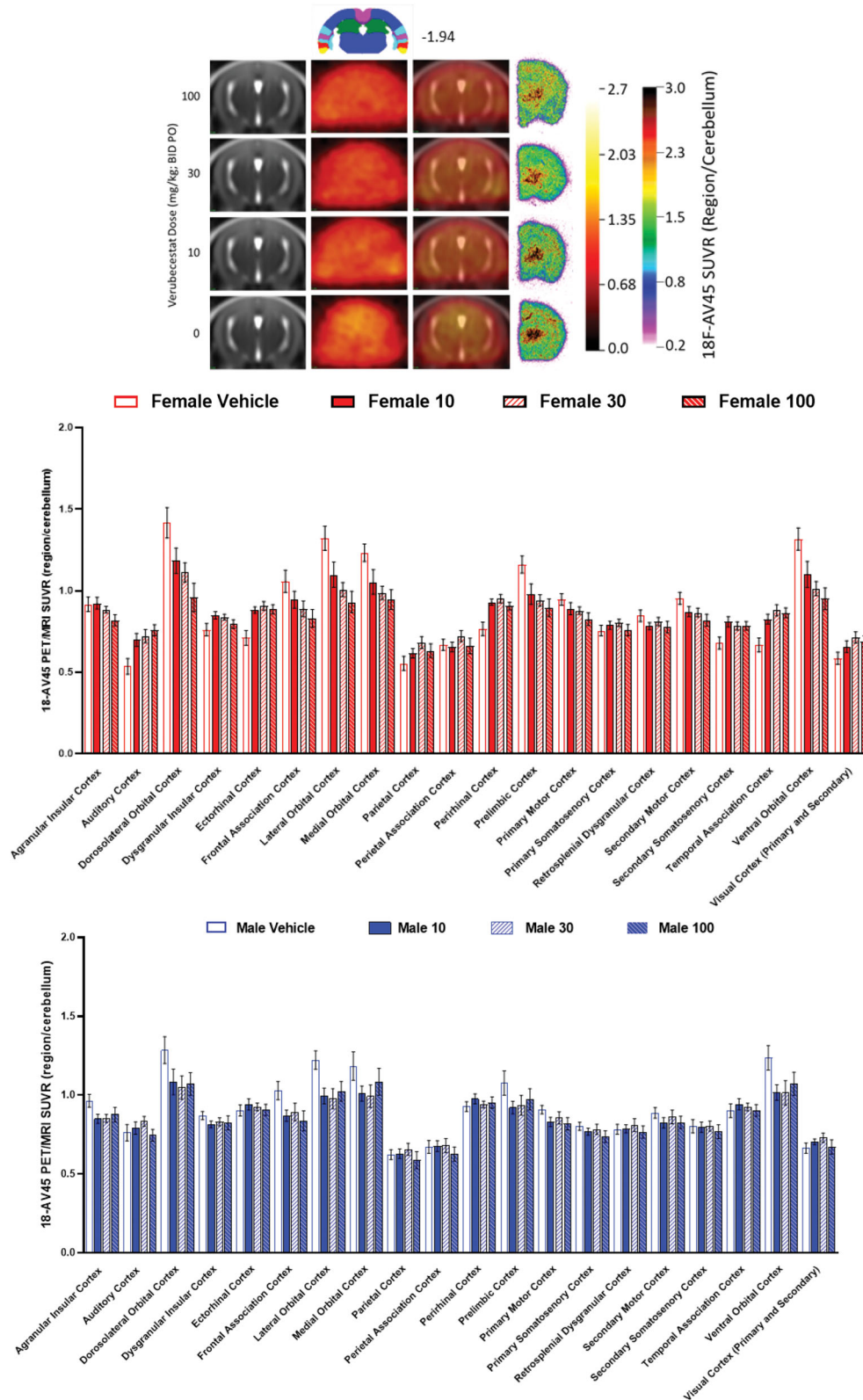


**FIGURE 2** Representative images for 18F-Flortetapir (AV45; Amyvid) (A) and autoradiography of  $n = 5$  randomly selected 6-month-old male and female 5XFAD mice following prophylactic verubecestat treatment. In all cases, images are presented as standard uptake volume ratio (SUVR) to the cerebellum. Representative bregma image panel presented as average magnetic resonance image (MRI) (left), positron emissions tomography (PET) (center-left), Fused (center-right), and Autoradiography (right) as a function of chronic verubecestat dosing (top to bottom). Quantitative analysis of 18F-AV45 uptake in male and female 5XFAD mice as a function of verubecestat dose. Data presented are means  $\pm$  1 standard error of the mean (SEM), and analyzed with a two-way analysis of variance (ANOVA), with sex and treatment as factors. As predicted, verubecestat (VER) produced dose-dependent reductions in 18F-AV45 uptake, which was regionally dependent (14 additional regions not presented did not show dose-related effects).

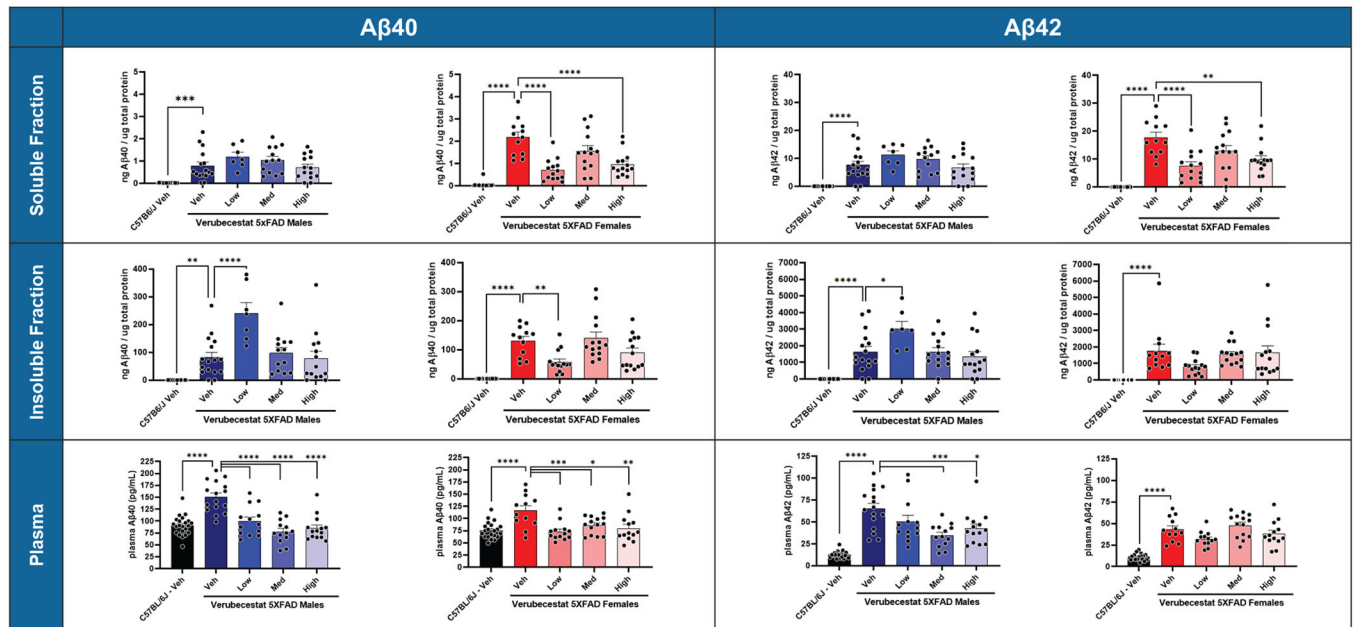


**FIGURE 3** Measurements of A $\beta$ 40 and A $\beta$ 42 following prophylactic treatment of verubecestat for 3 months in 6-month-old male and female 5XFAD mice. Soluble (top panel) and insoluble fractions (middle panel) from hemi-brain tissue homogenates, and plasma (bottom panel). Data presented as means with standard error of the mean (SEM) and individual data points plotted. Vehicle-treated 5XFAD compared to age- and sex-matched vehicle-treated C57BL6/J controls. Effects of verubecestat treatment in 5XFAD mice analyzed by one-way ANOVA versus 5XFAD vehicle control (\* $P < .05$ , \*\* $P < .01$ , \*\*\* $P < .005$ , \*\*\*\* $P < .001$ ). The A $\beta$  plasma effects of verubecestat are consistent with Villarreal et al.<sup>27</sup>.

### 3.4 | Verubecestat effects on the clinical and behavioral characteristics of 5XFAD mice

Coat color changes were observed  $\approx 2$  weeks from initiation of treatment and reported at all three sites. As illustrated in Figure 5, there was a dose-related increase in the robustness of coat color change ( $P < .05$  versus vehicle-treated 5XFAD) as quantified by the frailty index score.<sup>23</sup> No other measures of the frailty index were significantly altered by verubecestat treatment.

In the spontaneous alternation task, across the dose range tested, there was no effect of verubecestat treatment in male or female 5XFAD mice relative to age- and sex-matched controls at JAX, and these results were reproduced at PITT ( $P > .05$ ; Figure 5 and Figure S4). Although verubecestat treatment did not produce significant alterations in general locomotor or exploratory activity in the open field ( $P > .05$ ), dose-related reductions in latency to fall off the rotarod were observed in both male and female verubecestat-treated mice ( $P < .05$  versus within sex 5XFAD vehicle treated control; Figure 5D). The reduction in the ability to maintain balance resulting in increased fall frequency is indicative of motor impairment, which was observed initially in the JAX cohort (see Figure S4–S6), and reproduced in an independent cohort at PITT (see Figure S7–S9).

We conducted further analyses for A $\beta$  levels in the behavior cohort to understand if changes in PK or PD were associated with cognitive performance at the individual level, in the absence of an effect of treatment group (see Figure S10, Table S2). Although there was a modest improvement in males on hippocampal working memory, which was not

observed in females, the observed increase in percentage alternation was correlated with increasing exposure levels and not changes in A $\beta$  levels. Taken together these data suggest a potential non-specific effect of verubecestat (see transcriptomic analysis, Figure 6A)

### 3.5 | NanoString analysis

PCA of NanoString data revealed 5XFAD transgene as a main effect (Figure 6A). We observed a sex effect between male and female samples along the second principal components. Next, we fit a multiple linear regression model to identify genes with differential expression as a function of sex, dose, and 5XFAD genotype. Multiple linear regression analysis determined that most of the altered genes were significantly associated with sex and 5XFAD genotype, whereas 38 genes showed dose-related effects of treatment (Figure 6C–D, supplemental data). Both 5XFAD male and female mice, irrespective of verubecestat doses, exhibited significant positive correlations ( $P < .05$ ) with immune system-associated modules in Consensus Cluster B and neuroinflammation modules in Consensus Cluster C. Moreover, the higher doses of verubecestat in male 5XFAD mice resulted in a significant negative correlation ( $P < .05$ ) with cellular stress response and RNA metabolism-associated modules in Consensus Cluster E, suggesting anti-AD-related effects related to verubecestat treatment. Similarly, female verubecestat-treated 5XFAD mice displayed significant negative correlation ( $P < .05$ ) with several modules in Consensus Cluster E; however, effects were weaker relative to that of male 5XFAD mice



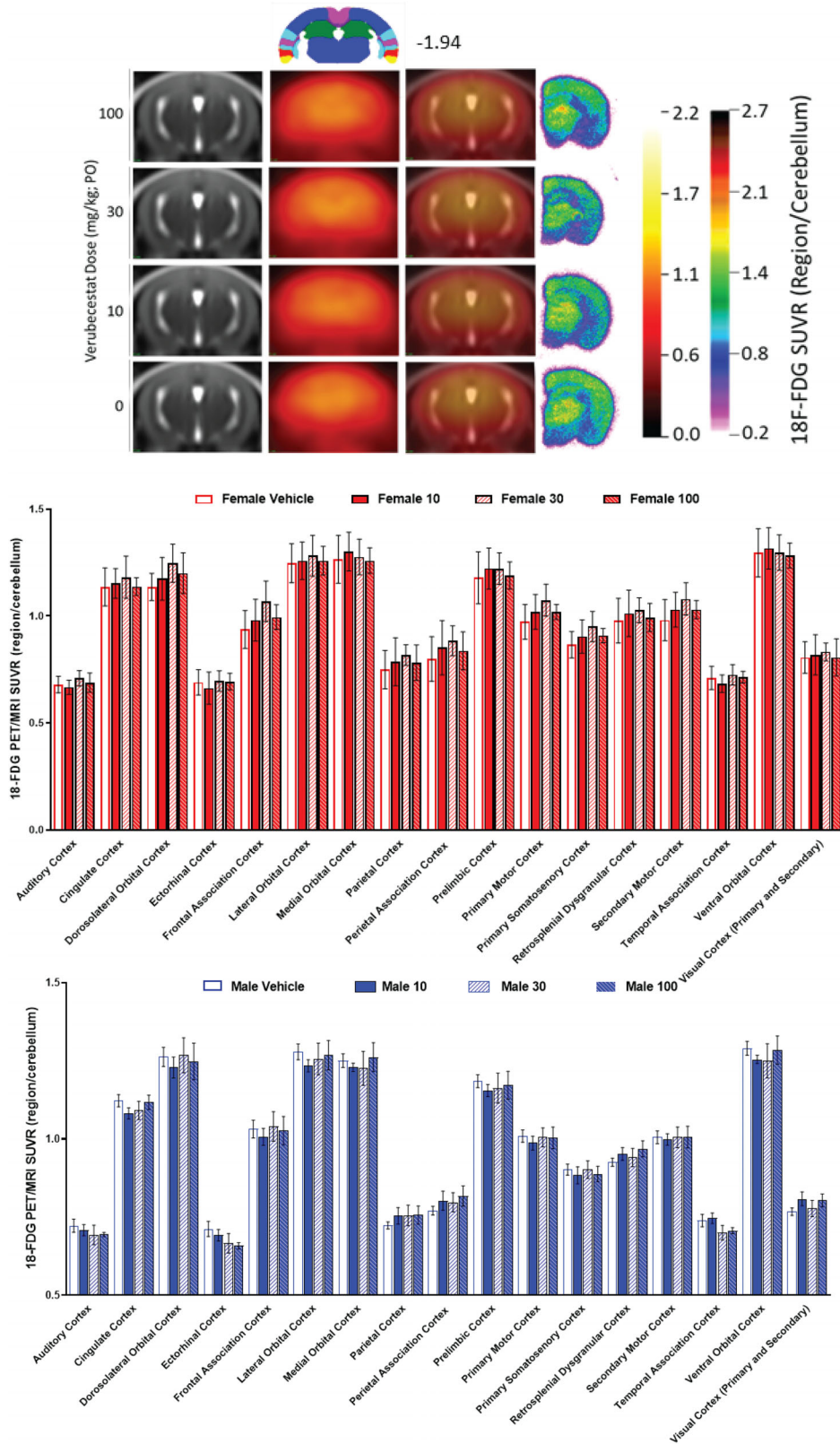


**FIGURE 4** Representative images for 18F-Fluorodeoxyglucose (FDG) positron emissions tomography/magnetic resonance imaging (PET/MRI) and autoradiography of  $n = 5$  randomly selected 6-month-old male and female 5XFAD mice following prophylactic verubecestat treatment. In all cases, images are presented as SUVR to the cerebellum. Representative bregma image panel presented as average MRI (left), PET (center-left), Fused (center-right), and Autoradiography (right) as a function of chronic verubecestat dosing (top to bottom). Quantitative analysis of 18F-FDG PET/MRI uptake in male and female 5XFAD mice as a function of verubecestat dose. Data presented are means  $\pm$  1 standard error of the mean (SEM), and analyzed with a two-way analysis of variance (ANOVA), with sex and treatment as factors. Verubecestat did not alter 18F-FDG uptake at any of the doses tested.

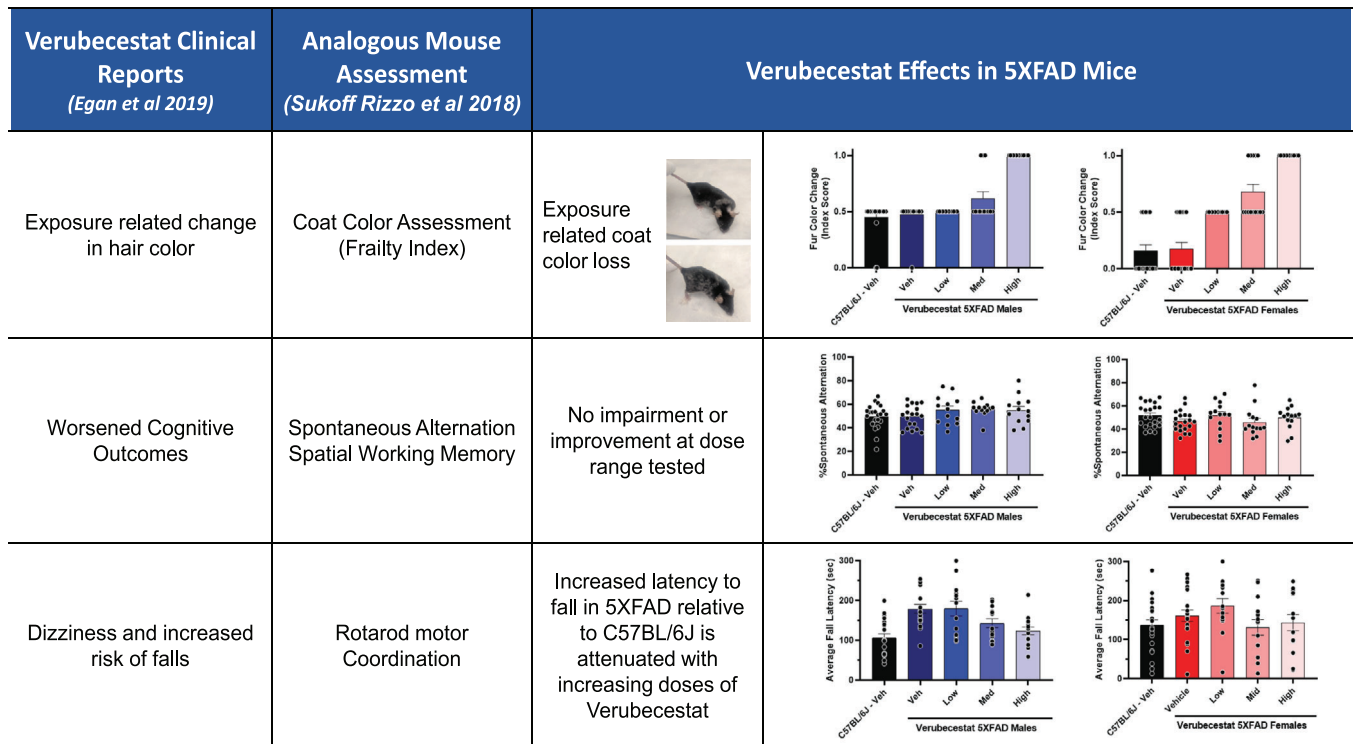


**FIGURE 5** Behavioral phenotypes of 6-month-old male and 5XFAD mice following chronic prophylactic treatment relative to age- and sex-matched vehicle-treated 5XFAD and vehicle-treated C57BL/6J wild-type controls. Verubecestat did not alter cognitive performance in 5XFAD mice at the dose range tested; however, side effects including coat color changes as measured by the frailty index and increased frequency of falls were observed and were dose related with treatment. These behavioral effects are consistent with the side effects reported for verubecestat in the clinic (Egan et al., 2018) at the same doses that were effective in attenuating amyloid deposition in the present study.

(Figure 6). Overall, we observed several anti-AD-related treatment effects; however, we did not observe any changes in immune- and neuronal-system-associated pathways for verubecestat treatment.

## 4 | DISCUSSION

Although verubecestat and other BACE-1 inhibitors have been unsuccessful in clinical trials to date due to safety and efficacy concerns, these trials have focused largely on treatment initiation in advanced stages of AD.<sup>7</sup> As BACE-1 inhibition functions to prevent A $\beta$  production as opposed to breaking down existing A $\beta$  aggregates, it is hypothesized that BACE-1 inhibition may be more effective as a prophylactic treatment for early-stage AD prior to the formation of A $\beta$  aggregates, or when the number of existing A $\beta$  aggregates is low.<sup>6-7</sup> Thus BACE-1 inhibitors may be beneficial for patients identified as at-risk for developing AD or those in early stages of AD. In this respect, to investigate the potential of a prophylactic approach, we utilized the tiered screening strategy of the MODEL-AD PTC.<sup>11</sup> We initiated treatment of the BACE-1 inhibitor verubecestat in a 5XFAD mouse model, at an age prior to the onset of significant A $\beta$  deposition.<sup>12</sup> We evaluated the drug formulation, stability, and in vivo PK and target tissue concentrations in 6-month-old male and female 5XFAD mice to align with the anticipated age- and AD-related disease pathology

at the conclusion of longitudinal treatment regimen. Previously we demonstrated<sup>11</sup> that plasma concentrations of verubecestat following oral gavage resulted in a short terminal half-life of  $\approx$ 2.5 hours, which would have required multiple daily oral gavage administration to maintain steady state levels. These data were critical for informing the dose regimen for the long-term chronic studies in chow formulated with verubecestat, which covered a concentration range of 10 to 100 mg/kg/day to capture sexually dimorphic exposures demonstrated in our pilot PK data, and in line with published effective concentration (EC50) values and the dosing regimen used in mouse models of amyloid deposition reported previously for verubecestat.<sup>24-25</sup>

In accordance with the MODEL-AD PTC pipeline, we prioritized translational outcome measures for these studies including 18F-AV45 and 18F-FDG PET/MRI. The 18F-AV45 PET/MRI assessments revealed a level of sensitivity far greater than that of bulk tissue fractionation and measurement via ELISA, with prophylactic verubecestat treatment demonstrating protective effects of amyloid accumulation in a dose-dependent manner. As with human AD, the distribution of amyloid plaques within the brain are heterogeneously distributed. In the case of the 5XFAD mouse model of AD, this distribution is highly localized to key brain regions such as the cortical, sub-cortical, thalamic, and pre-frontal regions.<sup>12</sup> This heterogeneous distribution of amyloid means that some regions of the brain will have high concentrations, as those previously listed, and some will have low levels of plaques.

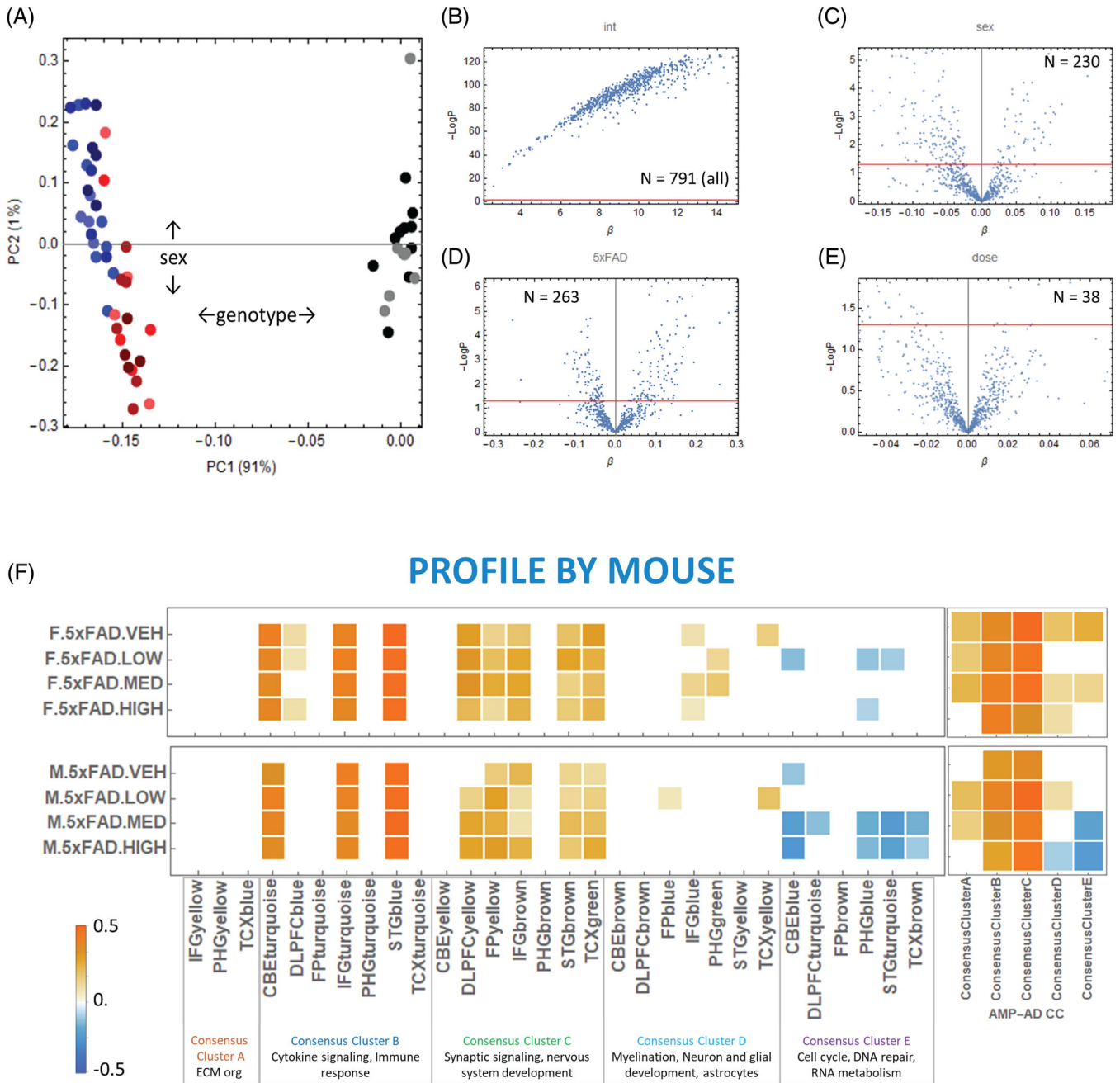


**FIGURE 6** Transcriptomic analysis of 5XFAD mice treated with verubecestat. (A) Principal component analysis (PCA) of NanoString transcriptomic data from all mouse models (5XFAD and WT control mice). The percent of variation explained by each principal component is displayed on the corresponding axis. WT female and male samples are represented with black and gray colors, respectively. The 5XFAD female samples are represented in blue shades; darker blue shades represent 5XFAD female samples treated with higher amount of verubecestat dose. Similarly, 5XFAD male samples are represented in red shades, with darker red shades representing 5XFAD male samples treated with a higher amount of verubecestat dose. (B–E) Multiple linear regression analysis of NanoString transcriptomics data using sex, the 5XFAD genotype, and dose as a dependent variable. Numbers in each panel (C,D) represent genes significantly associated with sex, 5XFAD, and dose, respectively. The x-axis represents effect (regression coefficients) and the y-axis represents corresponding statistical significant ( $-\log$  of  $p$ -values) for each gene. (E) Correlation analysis between mouse models and human data was performed for 30 Accelerating Medicines Partnership–Alzheimer’s Disease (AMP-AD) co-expression modules from postmortem brain regions. Gene expression changes in each mouse models were computed relative to sex-matched WT mice, which were correlated with change in expression in human cases versus controls. Significant positive correlations ( $P < .05$ ) are shown in red and negative correlations in blue.

The current treatment paradigm is a prophylactic model; this suggests that the treatment will prevent the accumulation of amyloid by inhibiting the  $\beta$ -site APP. As such, we would expect a dose-dependent decrease in amyloid as measured by 18F-AV45, and because of the heterogeneous distribution of amyloid production, we would expect and saw a non-uniform reduction in amyloid as a function of brain regions. Furthermore, due to verubecestat's mechanism of action, and the models heterogeneity, some regions that normally have high depositions, showed a much larger decrease in amyloid deposits with increasing dose, whereas in other regions, because of low deposition rates, these regions showed little to no change in amyloid changes with increasing dose. These data recapitulate the clinical findings for heterogeneous amyloid deposition in humans<sup>30,31</sup> and regional changes observed with BACE1 inhibitors.<sup>26</sup> Taken together, these data suggest that preclinical studies in animal models that include translational measurements such as in vivo PET/MR may have better predictive power than other ex vivo methods.

Related, plasma  $A\beta$  levels were reduced by prophylactic verubecestat treatment with greater reductions in  $A\beta_{40}$  than  $A\beta_{42}$ . These findings are consistent with previous reports in which verubecestat was determined to reduce the accumulation of  $A\beta_{40}$  to a greater extent than that of  $A\beta_{42}$ .<sup>25</sup> In contrast to the effects on amyloid deposition, prophylactic verubecestat treatment did not protect against alterations in glycolytic activity as measured by 18-FDG uptake. These data are consistent with a corresponding failure to improve cognitive performance of 5XFAD in the present study.

As a critical component of this study, we evaluated parameters related to the adverse effects experienced by patients treated with verubecestat in prior clinical trials in order to determine whether the initiation of verubecestat treatment would have similar effects in early stages of disease in an AD mouse model. The clinical observations included risk for falls and injuries, worsened cognitive outcomes, and changes in hair color.<sup>13-15</sup> The frailty index revealed changes in coat color in both male and female 5XFAD mice in a dose-dependent manner that were consistent with previous reports of hair color changes in humans receiving verubecestat, which is thought to result from BACE-2 inhibition.<sup>13-15</sup> Furthermore, 5XFAD verubecestat-treated mice exhibited increases in frequency of falls on the rotarod relative to vehicle-treated 5XFAD controls, which is in line with the increased falling risk observed in previous clinical trials.<sup>13-15</sup> Although cognitive performance was not worsened with prophylactic verubecestat treatment, the increase in side effects related to treatment implicates a narrow therapeutic window relative to the PD effects. It is possible that other BACE inhibitors may have an improved therapeutic window and should be explored using similar translational measures and analogous side-effect profiling.

A major limitation of the present study may be the 5XFAD model and its overexpression of amyloid that is likely well beyond physiologically relevant levels produced in patients with AD.<sup>12</sup> Improved model systems devoid of transgene-related overexpression may have better utility for exploring the effects of prophylactic treatment of BACE inhibitors to prevent or attenuate disease.

Another important observation was the effects of verubecestat treatment on gene expression signatures in 5XFAD mice. As reported previously, 5XFAD mice have transcriptomic signatures that capture a spectrum of gene-expression profiles of patients with AD.<sup>12</sup> The NanoString panel employed here revealed 38 genes that were modulated by verubecestat treatment in a dose-related manner. Transcriptomics data may therefore provide revealing information on verubecestat's mechanism of action at the molecular level. Related, transcriptomics may serve as an important tool for understanding the gaps in specific mechanisms of action in symptom and disease modification of drugs that could have translational power between animal models and patients. Furthermore, gene-expression signatures from patients and animal models could be aligned and used to best match the drug's transcriptomic signature with the potential of improving pre-clinical to clinical translation as well as success rates in the clinic by using this type of precision medicine approach for patient selection and stratification.

In conclusion, the present studies provide key insights into the potential utility of verubecestat as a prophylactic treatment for early intervention in AD and indicate that the adverse events associated with BACE inhibition at advanced stages of disease may be evident even when administered prior to significant disease, despite the potential neuroprotective effects from amyloid deposition.

#### ACKNOWLEDGMENT

The authors would like to acknowledge of The University of Pittsburgh Preclinical Phenotyping Core (PPC) Facility for behavioral phenotyping expertise and The Jackson Laboratory Center for Biometric Analysis (CBA).

#### CONFLICTS OF INTEREST

The authors are supported by funding from the National Institutes of Health, National Institute on Aging U54 AG054345. Dr. Oblak is supported by funding from the National Institute on Aging K01AG054753. BTL has served as a consultant for AvroBio and Eli-Lilly and is supported by additional funding: NIA R01 AG022304, RF1 AG051495, U54 AG065181, and U54 AG054345. Mass spectrometry and UV work was provided by the Clinical Pharmacology Analytical Core at Indiana University School of Medicine; a core facility supported by the IU Simon Cancer Center Support Grant P30 CA082709. A.L.O., Z.A.C., S.K.Q., R.P., C.B., A.R.M., K.D.O., L.H., K.J.K., J.A.M., J.P., S.C.P., A.A.B., K.E., R.S., G.L., S.P.W., B.N., A.O., M.S., G.R.H., G.W.C., H.W., B.T.L., P.R.T., and S.J.S.R. have no conflicts. Author disclosures are available in the supporting information.

#### REFERENCES

1. Jia J, Wei C, Chen S, et al. The cost of Alzheimer's disease in China and re-estimation of costs worldwide. *Alzheimers Dement*. 2018;14:483-491.
2. Citron M. Alzheimer's disease: strategies for disease modification. *Nat Rev Drug Discov*. 2010;9:387-398.
3. Karch CM, Cruchaga C, Goate AM. Alzheimer's disease genetics: from the bench to the clinic. *Neuron*. 2014;83:11-26.



4. Cummings J. Lessons learned from Alzheimer disease: clinical trials with negative outcomes. *Clin Transl Sci.* 2018;11:147-152.
5. Oxford AE, Stewart ES, Rohn TT. Clinical trials in Alzheimer's disease: a hurdle in the path of remedy. *Int J Alzheimers Dis.* 2020;2020:5380346.
6. Imbimbo BP, Watling M. Investigational BACE inhibitors for the treatment of Alzheimer's disease. *Expert Opin Investig Drugs.* 2019;28:967-975.
7. McDade E, Voytyuk I, Aisen P, et al. The case for low-level BACE1 inhibition for the prevention of Alzheimer disease. *Nat Rev Neurol.* 2021;17:703-714.
8. Hardy JA, Higgins GA. Alzheimer's disease: the amyloid cascade hypothesis. *Science.* 1992;256:184-185.
9. Roberds SL, Anderson J, Basi G, et al. BACE knockout mice are healthy despite lacking the primary beta-secretase activity in brain: implications for Alzheimer's disease therapeutics. *Hum Mol Genet.* 2001;10:1317-1324.
10. Zhang X, Fu Z, Meng L, He M, Zhang Z. The early events that initiate  $\beta$ -amyloid aggregation in Alzheimer's disease. *Front Aging Neurosci.* 2018;10:359.
11. Sukoff Rizzo SJ, Masters A, Onos KD, et al. Improving preclinical to clinical translation in Alzheimer's disease research. *Alzheimers Dement (N Y).* 2020;6:e12038.
12. Oblak AL, Lin PB, Kotredes KP, et al. Comprehensive evaluation of the 5XFAD mouse model for preclinical testing applications: a MODEL-AD study. *Front Aging Neurosci.* 2021;13:713726.
13. Egan MF, Kost J, Tariot PN, et al. Randomized trial of verubecestat for mild-to-moderate Alzheimer's disease. *N Engl J Med.* 2018;378:1691-1703.
14. Egan MF, Kost J, Voss T, et al. Randomized trial of verubecestat for prodromal Alzheimer's disease. *N Engl J Med.* 2019;380:1408-1420.
15. Egan MF, Mukai Y, Voss T, et al. Further analyses of the safety of verubecestat in the phase 3 EPOCH trial of mild-to-moderate Alzheimer's disease. *Alzheimers Res Ther.* 2019;11:68.
16. Oakley H, Cole SL, Logan S, et al. Intraneuronal beta-amyloid aggregates, neurodegeneration, and neuron loss in transgenic mice with five familial Alzheimer's disease mutations: potential factors in amyloid plaque formation. *J Neurosci.* 2006;26:10129-10140.
17. Percie du Sert N, Hurst V, Ahluwalia A, et al. The ARRIVE guidelines 2.0: updated guidelines for reporting animal research. *J Physiol.* 2020;598:3793-3801.
18. Soetaert K, Petzoldt T, Setzer RW. Solving differential equations in R: package deSolve. *J Stat Softw.* 2010;33:1-25.
19. Frese T, Rouze NC, Bouman CA, Sauer K, Hutchins GD. Quantitative comparison of FBP, EM, and Bayesian reconstruction algorithms for the IndyPET scanner. *IEEE Trans Med Imaging.* 2003;22:258-276.
20. Soon VC, Miller LM, Hutchins GD. A non-iterative method for emission tomographic image reconstruction with resolution recovery. Record: Nuclear Science Symposium Conference; 2007. p. 3468-3473.
21. Studholme C, Hill DL, Hawkes DJ. Automated three-dimensional registration of magnetic resonance and positron emission tomography brain images by multiresolution optimization of voxel similarity measures. *Med Phys.* 1997;24:25-35.
22. Franklin KBJ, Paxinos G. Paxinos and Franklin's The mouse brain in stereotaxic coordinates. Amsterdam, Academic Press, an imprint of Elsevier.
23. Tustison NJ, Avants BB, Cook PA, et al. N4ITK: improved N3 Bias Correction. *IEEE Trans Med Imaging.* 2010;29:1310-1320.
24. Yushkevich PA, Piven J, Hazlett HC, et al. User-guided 3D active contour segmentation of anatomical structures: significantly improved efficiency and reliability. *Neuroimage.* 2006;31:1116-1128.
25. Casali BT, Landreth GE. Abeta extraction from murine brain homogenates. *Bio Protoc.* 2016;6:e1787.
26. Kennedy ME, Stamford AW, Chen X, et al. The BACE1 inhibitor verubecestat (MK-8931) reduces CNS  $\beta$ -amyloid in animal models and in Alzheimer's disease patients. *Sci Transl Med.* 2016;8:363ra150.
27. Villarreal S, Zhao F, Hyde LA, et al. Chronic verubecestat treatment suppresses amyloid accumulation in advanced aged Tg2576-AbetaPPswe mice without inducing microhemorrhage. *J Alzheimers Dis.* 2017;59:1393-1413.
28. Lauro C, Limatola C. Metabolic reprogramming of microglia in the regulation of the innate inflammatory response. *Front Immunol.* 2020;11:493.
29. Xiang X, Wind K, Wiedemann T, et al. Microglial activation states drive glucose uptake and FDG-PET alterations in neurodegenerative diseases. *Sci Transl Med.* 2021;13:eabe5640.
30. Jeon S, Kang JM, Seo S, et al. Topographical heterogeneity of Alzheimer's disease based on MR imaging, tau PET, and amyloid PET. *Front Aging Neurosci.* 2019;11:211.
31. Fantoni E, Collij L, Alves IL, Buckley C, Farrar G. The Spatial-Temporal Ordering of Amyloid Pathology and Opportunities for PET Imaging. *J Nucl Med.* 2020;61:166-171.

## SUPPORTING INFORMATION

Additional supporting information can be found online in the Supporting Information section at the end of this article.

**How to cite this article:** Oblak AL, Cope ZA, Quinney SK, et al. Prophylactic evaluation of verubecestat on disease- and symptom-modifying effects in 5XFAD mice. *Alzheimer's Dement.* 2022;8:e12317. <https://doi.org/10.1002/trc2.12317>